

# Light-tunable charge density wave orders in MoTe<sub>2</sub> and WTe<sub>2</sub> single layers

Giovanni Marini<sup>1</sup> and Matteo Calandra<sup>2,1</sup>

<sup>1</sup>*Graphene Labs, Fondazione Istituto Italiano di Tecnologia, Via Morego, I-16163 Genova, Italy\**

<sup>2</sup>*Department of Physics, University of Trento, Via Sommarive 14, 38123 Povo, Italy*

By using constrained density functional theory modeling, we demonstrate that ultrafast optical pumping unveils hidden charge orders in group VI monolayer transition metal ditellurides. We show that irradiation of the insulating 2H phases stabilizes multiple transient charge density wave orders with light-tunable distortion, periodicity, electronic structure and bandgap. Moreover, optical pumping of the semimetallic 1T' phases generates a transient charge ordered metallic phase composed of 2D diamond clusters. For each transient phase we identify the critical fluence at which it is observed and the specific optical and Raman fingerprints to directly compare with future ultrafast pump-probe experiments. Our work demonstrates that it is possible to stabilize charge density waves even in insulating 2D transition metal dichalcogenides by ultrafast irradiation.

Designing and manipulating broken symmetry states with laser light is an appealing perspective as it can lead to the discovery of hidden ordered states and enable control over a broad range of material properties [1, 2]. Few layers transition metal dichalcogenides (TMDs) are an ideal class of materials for ultrafast investigations, mainly for two reasons. First, metallic dichalcogenides display the occurrence of competing orders such as charge density wave (CDW) phases and superconductivity. Second, insulating TMDs normally do not display charge ordering but have typical gaps in the 1 – 2.5 eV range[3], ideal for optical pumping. Inducing CDW in insulating dichalcogenides is important as it could lead to new low dimensional phases with unexpected topological and correlation properties.

Particularly relevant are MoTe<sub>2</sub> and WTe<sub>2</sub> as the barrier existing between the 2H and the 1T' phase is lower compared to the other compounds of the family [4]. The most stable MoTe<sub>2</sub> polytype is the 2H, however it has been shown that a transition towards the 1T' can be selectively activated in ultrathin layers by means of electrostatic doping [5], tensile strain [6] and laser irradiation [7]. Conversely, WTe<sub>2</sub> is stable in the 1T' polytype and the metastable 2H phase has been synthesized only recently [8, 9].

Most of the work carried out on irradiated MoTe<sub>2</sub> concerns the irreversible 2H-1T' phase transition. However, irreversible phase transitions are only a small part of the broken symmetry charge ordered states available after laser irradiation, as reversible transition towards transient phases can occur; these can be detected either by ultrafast X-ray diffraction at X-ray free electron laser facilities[10] or by pump-probe experiments to measure optical or Raman spectra after the electronic excitation[11, 12].

Phase transitions under ultrafast irradiation have been observed for conventional semiconductors under intense ultrafast irradiation[13, 14] (non-thermal melting), in phase-change materials[10] and have been proposed to occur in ferroelectrics [15]. However, in most of these cases, the ordered phase is present in the ground state and sup-

pressed by irradiation. Very few detections of hidden CDW orders (i.e. the ordered phase is a transient state induced by light) have been devised or demonstrated[16]. Furthermore, it is unclear if hidden orders are present in single layer dichalcogenides and at what fluence they can be observed.

In this work we demonstrate the occurrence of multiple charge ordered transient states in MoTe<sub>2</sub> and WTe<sub>2</sub> single layers after ultrafast irradiation of the 2H and 1T' phases in the high-excitation density regime ( $n_e \geq 10^{14} e^-/cm^2$ , where  $n_e$  represents the photocarrier concentration (PC)). Moreover we show the occurrence of a light-induced bandgap closing in the 2H phases. Finally, we identify specific spectroscopic fingerprints of each phase that will allow its detection in future ultrafast experiments. We investigate the effect of laser irradiation within density functional theory (DFT). In the case of insulators, we suitably constrain the occupations of the Kohn-Sham conduction eigenstates in order to mimic the thermalized photocarrier population. This approach has been described in Ref. [17] and we refer to it as constrained DFT (cDFT). We implemented the cDFT technique as well as the calculation of forces and stress tensor in the presence of an electron-hole plasma within the Quantum ESPRESSO distribution[18, 19]. In the case of metals and semimetals (1T' phases), the radiative electron-hole recombination is fast[20, 21], thus laser excitation is simulated employing Fermi-Dirac occupations at high temperature. All the simulation details are reported in the Supplemental Material (SM), which includes Refs.[22–52].

The main results of our paper are summarized in Figs. 1,2. First, we find that light induces a progressive formation of CDW order in 2H-MoTe<sub>2</sub> (and 2H-WTe<sub>2</sub>), starting already at  $n_e = 0.1 e^-$  per formula unit (*f.u.*). The hidden CDW order, labeled 2H', arises from an imaginary phonon frequency in correspondence to the M-point of the Brillouin zone (BZ) and involves clustering of three Mo atoms (the soft phonon pattern involves the displacement of Mo atoms only, see Fig. 2 (b)). The 2H' phase is in turn prone to structural instabilities, in

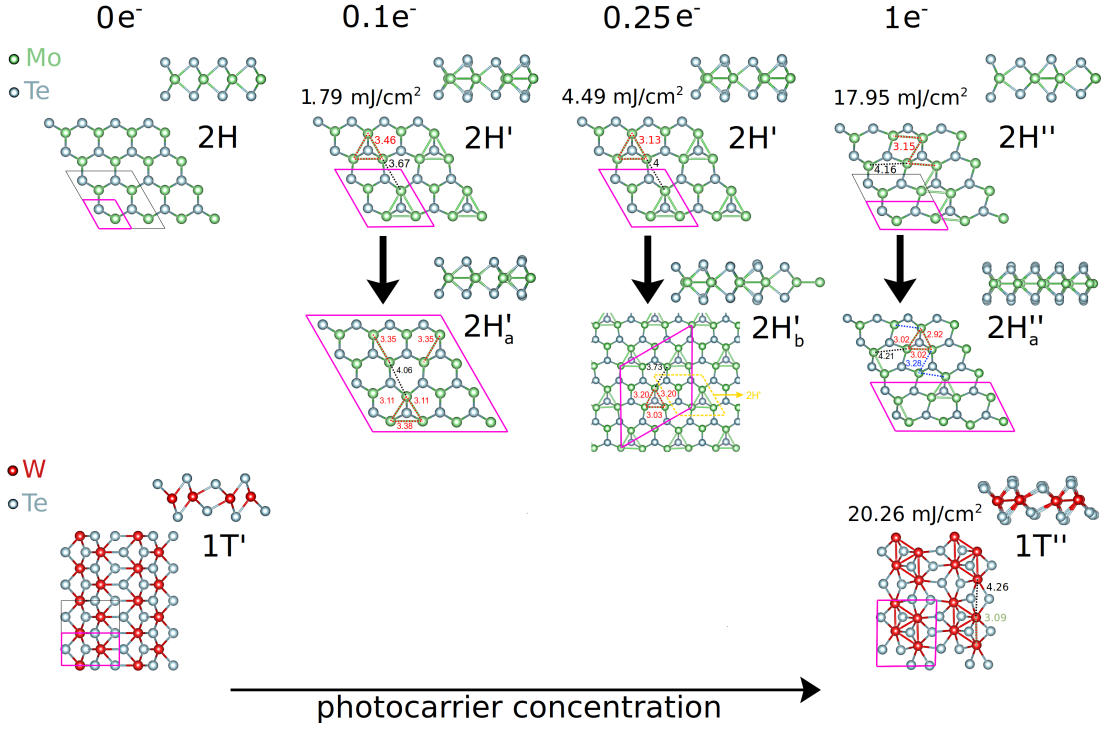


FIG. 1. Schematic representation of hidden orders in monolayer dichalcogenides. Upper panel: 2H-MoTe<sub>2</sub> as a function of the PC (*f.u.*). Mo clusterization is represented by green bonds. At  $n_e = 0.25 e^-/f.u.$  ( $n_e = 1 e^-/f.u.$ ) the energy gain associated to the 2H  $\rightarrow$  2H' (2H  $\rightarrow$  2H'') distortion is 107.2 (583.1) meV/*f.u.*, while the 2H'  $\rightarrow$  2H'<sub>b</sub> (2H''  $\rightarrow$  2H'<sub>a</sub>) distortion has an energy gain of only 3.1 (6.6) meV/*f.u.*. Lower panel: 1T'-WTe<sub>2</sub> as a function of the PC (*f.u.*). Numbers in the crystal structure images represent atomic distances in Å. For the relation between fluence and PC see SM.

particular two lower symmetry phases compete; we refer to them as 2H'<sub>a</sub> and 2H'<sub>b</sub>. Most importantly, the 2H' phase, and the derived *a* and *b* distorted structures, display a progressive bandgap closing with increasing PC and transition to a metallic state at  $n_e = 0.25 e^-/f.u.$  (see Figs. 2 (d),(e)). At  $n_e = 1 e^-/f.u.$  (still reachable by current laser sources) a new  $2 \times 1$  CDW appears, composed of alternating anisotropically compressed and expanded stripes of hexagons. We label this phase 2H''. The 2H'' phase is in turn unstable and relaxes towards a lower symmetry structure, named 2H''<sub>a</sub> phase.

Second, pumping on top of the 1T'-MoTe<sub>2</sub> and 1T'-WTe<sub>2</sub> phases at  $n_e \approx 1 e^-/f.u.$  stabilizes a  $2 \times 2$  hidden CDW order composed of 2D diamond clusters of transition metal atoms (see Fig. 1 bottom right), that we label 1T''. In the absence of optical pumping, this CDW structure has been found as metastable and competing with the 1T' phase in MoS<sub>2</sub>[53] and has been occasionally detected in some MoS<sub>2</sub> single layers[54]. Thus, laser light can be used to reveal hidden charge density wave orders, hard to stabilize in standard thermochemical conditions. Finally, we note that energy transfer from the electrons to the lattice could reduce the effective temperature to be considered in the simulations, suggesting that the critical PC for the stabilization of the 1T'' phase is somewhat underestimated.

We now study the mechanism destabilizing the 2H structures in detail (for the analysis of the CDW formation in 1T' phases see SM). We consider MoTe<sub>2</sub>, but similar results for WTe<sub>2</sub> are shown in the SM. We perform supercell finite difference calculations of the phonon frequencies at specific high-symmetry points. The results are plotted in Fig. 2 ((a), (b), (c)). Raman active phonons at  $\Gamma$  are plotted in red. At low PCs, in a single-valley direct gap semiconductor, momentum and energy conservation enforce that only zone center phonons can be excited. Typically, if free internal coordinates are present, this results in displacive excitation of coherent Raman phonons. MoTe<sub>2</sub> is a two-valley semiconductor and phonon excitations at  $\Gamma$  and  $\mathbf{K}$  are both possible. As it can be seen in Fig.2 (a) the  $A'_1$  mode softens under weak photoexcitation. Recently it was suggested that phonon softenings at  $\Gamma$  drive the irreversible 2H-1T' transition in monolayer MoTe<sub>2</sub>[55]. However, we find that even at large PCs  $\Gamma$  frequencies never become imaginary (Fig. 2(a)), invalidating this claim. We find that a critical PC of  $n_e \approx 1.75 e^-/f.u.$ , corresponding to a high fluence of 31.41 mJ/cm<sup>2</sup>, is needed to destabilize  $\Gamma$  phonons, suggesting that other concomitant mechanisms such as Te vacancy creation are involved in the irreversible 2H $\rightarrow$ 1T' transition [56]. At higher PCs instabilities can also occur at other phonon momenta. Already

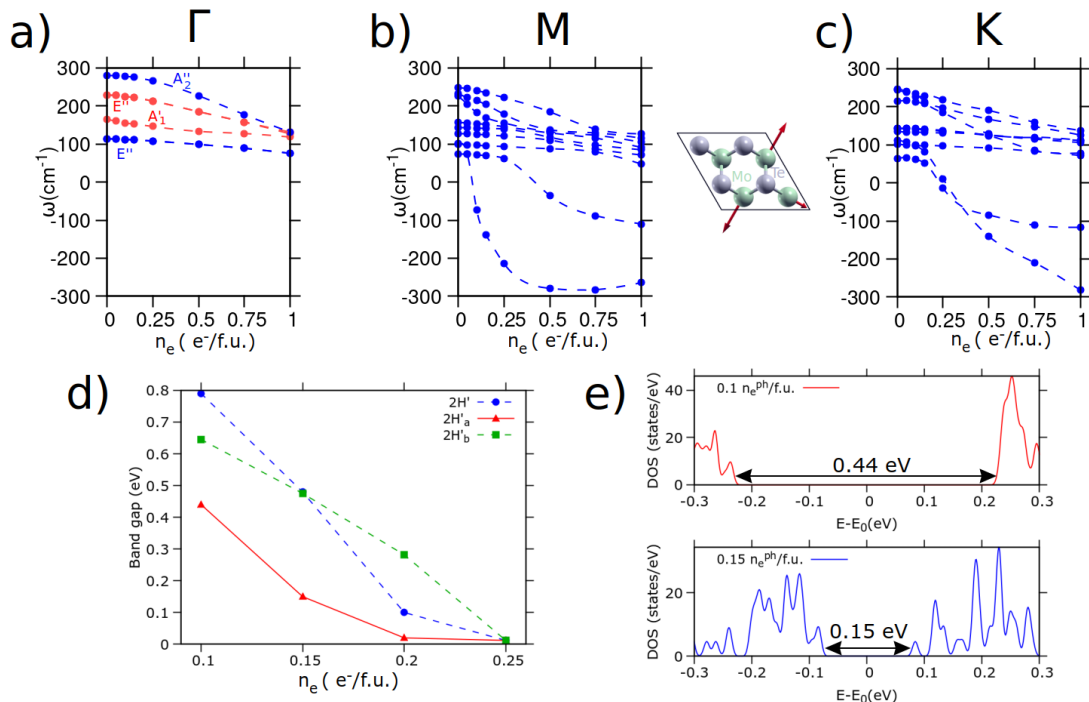


FIG. 2. Panels a,b,c: Phonon frequencies as a function of PC for 2H-MoTe<sub>2</sub> at  $\Gamma$ ,  $M$ ,  $K$  points of the BZ, respectively. Raman active modes at  $\Gamma$  are depicted in red. The lowest eigenvector at the  $M$ -point is schematically depicted in panel b. Panel d: electronic bandgap as a function of PC. Panel e: density of states for the  $2H'_a$  phase of MoTe<sub>2</sub> at  $n_e = 0.1$  and  $0.15 e^-/f.u.$ .

at  $n_e = 0.1 e^-/f.u.$ ,  $M$ -point phonons are strongly imaginary. In order to understand the mechanism responsible for the formation of the  $2H'$  phases and to decouple the role of conduction and valence states in the CDW formation we also calculate the phonon frequency spectrum within a rigid doping approximation, simulating an electron charge excess or deficiency. The rigid doping calculations show that both conduction and valence states contribute to the  $M$ -point phonon softening observed in cDFT (see Fig. S7 of SM).

As mentioned earlier, both  $2H'$  and  $2H''$  phases present additional structural instabilities (see Figs. S8, S9 of SM). Concerning the  $2H'$ , we observe a competition between a  $4 \times 4$  ( $2H'_a$ ) and  $2\sqrt{3} \times 2\sqrt{3}$  ( $2H'_b$ ) periodical distortion. The  $2H'_a$  phase is more stable for  $0.1 e^-/f.u. \leq n_e \leq 0.2 e^-/f.u.$ , while the  $2H'_b$  is more stable at  $n_e = 0.25 e^-/f.u.$ . At  $n_e = 1 e^-/f.u.$ , the  $2H''$  instability (Fig. S5 of the SM, bottom right panel) leads to the  $2H''_a$  phase, having a  $4 \times 2$  periodicity. This further distortion produces an energy gain of  $6.6 \text{ meV}/f.u.$  with respect to the  $2H''$  phase. We underline that the  $2H' \rightarrow 2H'_b$  and  $2H'' \rightarrow 2H''_a$  represent minor distortions relatively to the  $2H \rightarrow 2H'$  and  $2H \rightarrow 2H''$  distortions respectively, as demonstrated by the relative energy gain: at  $n_e = 0.25 e^-/f.u.$  we calculate an energy gain of  $107.2 \text{ meV}/f.u.$  for the  $2H \rightarrow 2H'$  distortion against an energy gain of  $3.1 \text{ meV}/f.u.$  for the  $2H' \rightarrow 2H'_b$  distortion; similarly, at  $n_e = 1 e^-/f.u.$  we calculate an energy gain of

$583.1 \text{ meV}/f.u.$  for the  $2H \rightarrow 2H''$  distortion against  $6.6 \text{ meV}/f.u.$  for the  $2H'' \rightarrow 2H''_a$  distortion. Whereas, this is not the case for the  $2H'_a$  phase: at  $n_e = 0.15 e^-/f.u.$  we calculate comparable energy gains for the  $2H \rightarrow 2H'$  ( $\approx 20 \text{ meV}/f.u.$ ) and the  $2H' \rightarrow 2H'_a$  distortion ( $\approx 29 \text{ meV}/f.u.$ ).

Having understood the mechanism leading to CDW formation, we identify possible spectroscopic signatures of the transient phases. In the case of the  $2H'$  and  $2H''$  structures, we calculate the imaginary part of the dielectric function  $\epsilon(\omega)$  allowing both for valence to valence and conduction to conduction optical transitions (absent in the ground state) on top of the valence to conduction ones. In Fig.3 (a), we consider both  $2H'$ ,  $2H''$  phases (solid lines) and their respective distortions (dashed lines) at  $n_e = 0.25$  and  $1 e^-/f.u.$  (see also Fig. S10 of SM). For the ground state (i.e. no pumping), our results (see Figs. S11,S12 of SM) are in good agreement with previously published *ab-initio* results[59][60]. The excited state configuration displays a metallic behaviour (Drude peak) both in MoTe<sub>2</sub> and WTe<sub>2</sub> (see Fig. 3 (a) for MoTe<sub>2</sub> and Figs. S11-S14 of SM for WTe<sub>2</sub> as well as data on reflectance, energy loss and decomposition of  $\text{Im}\{\epsilon(\omega)\}$  over optical transitions), which can be recognized from the low-frequency divergence of  $\epsilon(\omega)$ . This is related to the occurrence of an electron-hole plasma. The main changes in the dielectric function with increasing PC are observed below 2 eV. In par-

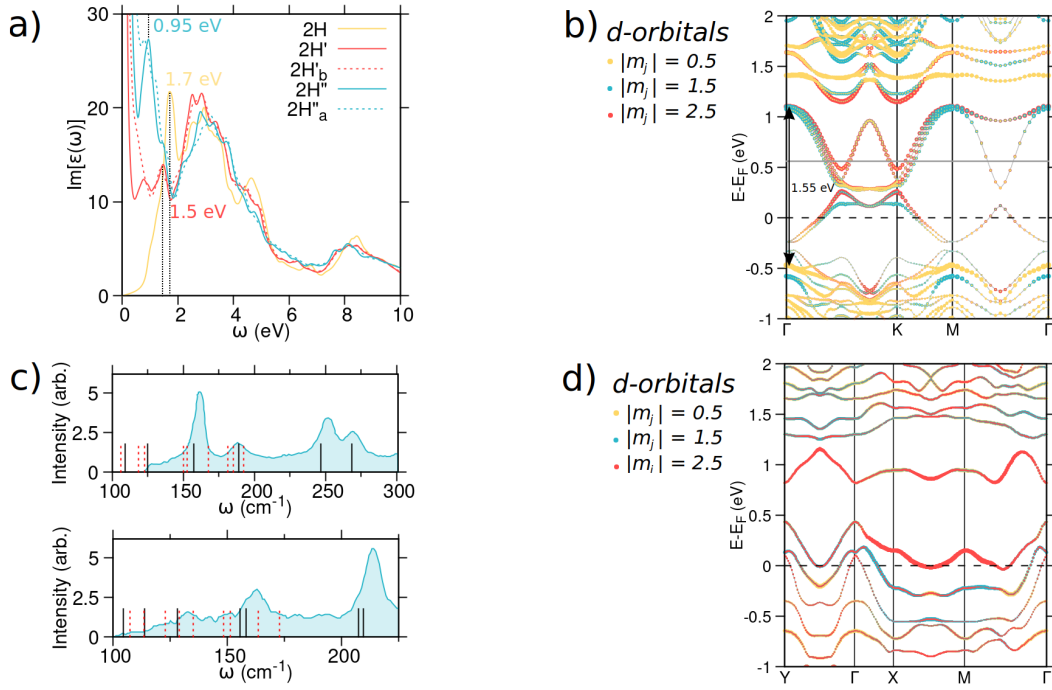


FIG. 3. Panel a: Imaginary part of  $\epsilon(\omega)$  evaluated at  $n_e = 0, 0.25$  and  $1 e^-/f.u.$  for 2H-MoTe<sub>2</sub> and its distorted phases. Panel b: Kohn-Sham eigenvalues along the 2H high symmetry BZ path for 2H' MoTe<sub>2</sub> at  $n_e = 0.25 e^-/f.u.$ , projected onto atomic  $d$ -orbitals. Black dashed line (grey line) represents the valence (conduction) *quasi*-Fermi level. Panel c: Calculated Raman frequencies (black lines) for 1T'-MoTe<sub>2</sub> (top) and WTe<sub>2</sub> (bottom), compared with the experimental Raman spectrum (cyan shaded region) for 1T'-MoTe<sub>2</sub>[57] and 1T'-WTe<sub>2</sub>[58]. Red dashed lines represent the Raman frequencies of the 1T'' phase at  $n_e = 1 e^-/f.u.$ . Panel d: Kohn-Sham eigenvalues along the 1T' high symmetry BZ path for 1T''-WTe<sub>2</sub> at  $n_e = 1 e^-/f.u.$ , projected onto atomic  $d$ -orbitals.

ticular, the peak observed in the ground state at 1.7 eV, attributed to the valence-conduction optical transition (Fig. S4 of SM, black arrow), is red-shifted to 1.5 eV at  $n_e = 0.25 e^-/f.u.$ , as expected observing the corresponding electronic transition at the  $\Gamma$ -point (see Fig. 3 (b)). Furthermore, its intensity is notably reduced. At  $n_e = 1 e^-/f.u.$  this peak is absent, while a new peak at 0.95 eV not directly related to the valence-conduction contribution appears. Thus, monitoring the evolution of the peak detected at 1.7 eV in the ground state as a function of the PC is equivalent to track the bandgap closing. The  $2H'_a$ ,  $2H'_b$  and  $2H''_a$  distortions slightly modify the optical response of the parent structures (see Fig. S10 of SM), causing a small red-shift of the 1.5 eV peak for the case of 2H' phase (down to 1.45 eV) and of the 0.95 eV peak (down to 0.89 eV) for the 2H'' phase and changing the Drude peak intensity.

For what concerns the 1T' and 1T'' phases, a clear distinction between the two occurs in Raman spectra. The calculated Raman frequencies are shown in Fig.3 (c) for 1T'-MoTe<sub>2</sub> and 1T'-WTe<sub>2</sub>, and for photoexcited 1T''-MoTe<sub>2</sub> and 1T''-WTe<sub>2</sub>. Those are compared to the experimental ground state Raman data from Refs. [57, 58]. For 1T'-MoTe<sub>2</sub>, the agreement between theory and experiments is excellent. For the 1T'-WTe<sub>2</sub> phase an over-

all red-shift ( $\approx 2-3\%$  of the value) of the phonon frequencies with respect to the experiment occurs, consistently with previous calculations[61] (see Tab. S4 and the discussion in the SM). We focus on the highest-energy most intense peaks (above 225 cm<sup>-1</sup> for 1T'-WTe<sub>2</sub> and above 200 cm<sup>-1</sup> for 1T'-MoTe<sub>2</sub>), due to phonon modes of  $A_{1g}$  and  $A_{2g}$  symmetries. The two peaks are well separated in 1T'-MoTe<sub>2</sub> and they are strongly overlapping in 1T'-WTe<sub>2</sub>, in good agreement with what found in experiments, demonstrating the reliability of our Raman calculations. In the 1T'' phase these two modes are completely absent. Thus, the structural transition is marked by the disappearance of these peaks in both compounds. The calculated Kohn-Sham eigenvalues for 1T''-WTe<sub>2</sub> are depicted in Fig.3 (d): a completely different band structure with respect to 1T'-WTe<sub>2</sub> is observed (see also Figs. S17,S18 of SM).

In conclusion, by using first principles calculations we have shown that light can be used to unveil hidden CDW order in the transient states of MoTe<sub>2</sub> and WTe<sub>2</sub> phases. Pumping on the 2H phases leads first to the stabilization of the  $2H'_a$  CDW ( $4 \times 4$  spatial periodicity), then to the  $2H'_b$  CDW ( $2\sqrt{3} \times 2\sqrt{3}$  periodicity), and finally to the  $2H''_a$  phase ( $4 \times 2$  periodicity). Most important, the  $2H'_a$  reconstruction shows an electronic gap that is pro-

gressively reduced as a function of fluence, showing a light tunable bandgap closing. Thus, inducing a photo-carrier population in the 2H-MoTe<sub>2</sub> leads to the following successive transitions: 2H (insulating, no-CDW) → 2H'<sub>a</sub> (gapped, 4×4 CDW) → 2H'<sub>b</sub> (gapless, 2×2 CDW) → 2H''<sub>a</sub> (gapless 4×2). Given the similar results obtained for MoTe<sub>2</sub> and WTe<sub>2</sub>, we speculate that similar 2H → 2H' → 2H'' structural transformations occur in other 2D insulating dichalcogenides. We also show that pumping on the 1T' at  $n_e = 1 e^-/f.u.$  leads to the transient distorted 1T'' phase. This new structure is characterized by diamond shaped Mo(W) clusters and a 2×2 periodicity. For each hidden order we identify the spectroscopic fingerprints paving the way to ultrafast measurements of transient states in monolayer dichalcogenides.

Finally, we have shown that the charge ordered phases occurring after laser irradiation are different from those commonly observed in the ground state of metallic transition metal dichalcogenides, such as NbSe<sub>2</sub> or TiSe<sub>2</sub>. Our work opens to the detection of new unexpected structural instabilities in this family of compounds.

We acknowledge support from the European Union's Horizon 2020 research and innovation programme Graphene Flagship under grant agreement No 881603. We acknowledge the CINECA award under the ISCRA initiative, for the availability of high performance computing resources and support. We acknowledge PRACE for awarding us access to Joliot-Curie at GENCI@CEA, France (project file number 2021240020).

---

\* giovanni.marini@iit.it

- [1] J. Lloyd-Hughes, P. Oppeneer, T. P. dos Santos, A. Schleife, S. Meng, M. A. Sentef, M. Ruggenthaler, A. Rubio, I. Radu, M. Murnane, X. Shi, H. Kapteyn, B. Stadtmüller, K. M. Dani, F. da Jornada, E. Prinz, M. Aeschlimann, R. Milot, M. Burdanova, J. Boland, T. L. Cocker, and F. A. Hegmann, *Journal of Physics: Condensed Matter* (2021).
- [2] M. Maiuri, M. Garavelli, and G. Cerullo, *Journal of the American Chemical Society* **142**, 3 (2020), pMID: 31800225, <https://doi.org/10.1021/jacs.9b10533>.
- [3] F. A. Rasmussen and K. S. Thygesen, *The Journal of Physical Chemistry C* **119**, 13169 (2015), <https://doi.org/10.1021/acs.jpcc.5b02950>.
- [4] X. Qian, J. Liu, L. Fu, and J. Li, *Science* **346**, 1344 (2014), <https://science.sciencemag.org/content/346/6215/1344>.
- [5] Y. Wang, J. Xiao, H. Zhu, Y. Li, Y. Alsaïd, K. Y. Fong, Y. Zhou, S. Wang, W. Shi, Y. Wang, A. Zettl, E. J. Reed, and X. Zhang, *Nature* **550**, 487 (2017).
- [6] S. Song, D. H. Keum, S. Cho, D. Perello, Y. Kim, and Y. H. Lee, *Nano Letters* **16**, 188 (2016), pMID: 26713902, <https://doi.org/10.1021/acs.nanolett.5b03481>.
- [7] S. Cho, S. Kim, J. H. Kim, J. Zhao, J. Seok, D. H. Keum, J. Baik, D.-H. Choe, K. J. Chang, K. Suenaga, S. W. Kim, Y. H. Lee, and H. Yang, *Science* **349**, 625 (2015), <https://science.sciencemag.org/content/349/6248/625>.
- [8] S. Li, F.-c. Lei, X. Peng, R.-q. Wang, J.-f. Xie, Y.-p. Wu, and D.-s. Li, *Inorganic Chemistry* **59**, 11935 (2020), pMID: 32815362, <https://doi.org/10.1021/acs.inorgchem.0c02049>.
- [9] M. S. Sokolikova and C. Mattevi, *Chem. Soc. Rev.* **49**, 3952 (2020).
- [10] E. Matsubara, S. Okada, T. Ichitsubo, T. Kawaguchi, A. Hirata, P. F. Guan, K. Tokuda, K. Tanimura, T. Matsunaga, M. W. Chen, and N. Yamada, *Phys. Rev. Lett.* **117**, 135501 (2016).
- [11] C. Ferrante, A. Virga, L. Benfatto, M. Martinati, D. De Fazio, U. Sassi, C. Fasolato, A. K. Ott, P. Postorino, D. Yoon, G. Cerullo, F. Mauri, A. C. Ferrari, and T. Scopigno, *Nature Communications* **9**, 308 (2018).
- [12] L. Huang, J. P. Callan, E. N. Glezer, and E. Mazur, *Phys. Rev. Lett.* **80**, 185 (1998).
- [13] C. W. Siders, *Science* **286**, 1340 (1999).
- [14] A. Rousse, C. Rischel, S. Fourmaux, I. Uschmann, S. Sebban, G. Grillon, P. Balcou, E. Förster, J. Geindre, P. Audebert, J. Gauthier, and D. Hulin, *Nature* **410**, 65 (2001).
- [15] C. Paillard, E. Torun, L. Wirtz, J. Íñiguez, and L. Bellaïche, *Phys. Rev. Lett.* **123**, 087601 (2019).
- [16] A. Kogar, A. Zong, P. E. Dolgirev, X. Shen, J. Straquadine, Y.-Q. Bie, X. Wang, T. Rohwer, I.-C. Tung, Y. Yang, R. Li, J. Yang, S. Weathersby, S. Park, M. E. Kozina, E. J. Sie, H. Wen, P. Jarillo-Herrero, I. R. Fisher, X. Wang, and N. Gedik, *Nature Physics* **16**, 159 (2020).
- [17] P. Tangney and S. Fahy, *Phys. Rev. B* **65**, 054302 (2002).
- [18] P. Giannozzi, S. Baroni, N. Bonini, M. Calandra, R. Car, C. Cavazzoni, D. Ceresoli, G. L. Chiarotti, M. Cococcioni, I. Dabo, A. D. Corso, S. de Gironcoli, S. Fabris, G. Fratesi, R. Gebauer, U. Gerstmann, C. Gougoussi, A. Kokalj, M. Lazzeri, L. Martin-Samos, N. Marzari, F. Mauri, R. Mazzarello, S. Paolini, A. Pasquarello, L. Paulatto, C. Sbraccia, S. Scandolo, G. Sclauzero, A. P. Seitsonen, A. Smogunov, P. Umari, and R. M. Wentzcovitch, *Journal of Physics: Condensed Matter* **21**, 395502 (2009).
- [19] P. Giannozzi, O. Baseggio, P. Bonfà, D. Brunato, R. Car, I. Carnimeo, C. Cavazzoni, S. de Gironcoli, P. Delugas, F. Ferrari Ruffino, A. Ferretti, N. Marzari, I. Timrov, A. Urru, and S. Baroni, *The Journal of Chemical Physics* **152**, 154105 (2020), <https://doi.org/10.1063/5.0005082>.
- [20] F. Schmitt, P. S. Kirchmann, U. Bovensiepen, R. G. Moore, L. Rettig, M. Krenz, J.-H. Chu, N. Ru, L. Perfetti, D. H. Lu, M. Wolf, I. R. Fisher, and Z.-X. Shen, *Science* **321**, 1649 (2008), <https://science.sciencemag.org/content/321/5896/1649>.
- [21] M. Hajlaoui, E. Papalazarou, J. Mauchain, G. Lantz, N. Moisan, D. Boschetto, Z. Jiang, I. Miotkowski, Y. P. Chen, A. Taleb-Ibrahimi, L. Perfetti, and M. Marsi, *Nano Letters* **12**, 3532 (2012), pMID: 22658088, <https://doi.org/10.1021/nl301035x>.
- [22] P. Scherpelz, M. Govoni, I. Hamada, and G. Galli, *Journal of Chemical Theory and Computation* **12**, 3523 (2016), pMID: 27331614, <https://doi.org/10.1021/acs.jctc.6b00114>.
- [23] J. P. Perdew, K. Burke, and M. Ernzerhof, *Physical Review Letters* **77**, 3865 (1996).
- [24] H. J. Monkhorst and J. D. Pack, *Physical Review B* **13**, 5188 (1976).
- [25] C. H. Naylor, W. M. Parkin, Z. Gao, H. Kang, M. Noyan, R. B. Wexler, L. Z. Tan, Y. Kim, C. E. Kehayias,

- F. Streller, Y. R. Zhou, R. Carpick, Z. Luo, Y. W. Park, A. M. Rappe, M. Drndić, J. M. Kikkawa, and A. T. C. Johnson, *2D Materials* **4**, 021008 (2017).
- [26] M. Kan, H. G. Nam, Y. H. Lee, and Q. Sun, *Phys. Chem. Chem. Phys.* **17**, 14866 (2015).
- [27] J. Heyd, G. E. Scuseria, and M. Ernzerhof, *The Journal of Chemical Physics* **118**, 8207 (2003), <https://doi.org/10.1063/1.1564060>.
- [28] J. Heyd and G. E. Scuseria, *The Journal of Chemical Physics* **121**, 1187 (2004), <https://doi.org/10.1063/1.1760074>.
- [29] A. Splendiani, L. Sun, Y. Zhang, T. Li, J. Kim, C.-Y. Chim, G. Galli, and F. Wang, *Nano Letters* **10**, 1271 (2010), pMID: 20229981, <https://doi.org/10.1021/nl903868w>.
- [30] L. Yuan and L. Huang, *Nanoscale* **7**, 7402 (2015).
- [31] A. Chernikov, C. Ruppert, H. M. Hill, A. F. Rigosi, and T. F. Heinz, *Nature Photonics* **9**, 466 (2015).
- [32] H. Haug and S. W. Koch, *Quantum Theory of the Optical and Electronic Properties of Semiconductors*, 5th ed. (WORLD SCIENTIFIC, 2009) <https://www.worldscientific.com/doi/pdf/10.1142/7184>.
- [33] M. Palumbo, M. Bernardi, and J. C. Grossman, *Nano Letters* **15**, 2794 (2015), pMID: 25798735, <https://doi.org/10.1021/nl503799t>.
- [34] S. Pan, W. Kong, J. Liu, X. Ge, P. Zereshki, S. Hao, D. He, Y. Wang, and H. Zhao, *ACS Applied Nano Materials* **2**, 459 (2019), <https://doi.org/10.1021/acsanm.8b02008>.
- [35] G. Froehlicher, E. Lorchat, and S. Berciaud, *Phys. Rev. B* **94**, 085429 (2016).
- [36] C. Ruppert, O. B. Aslan, and T. F. Heinz, *Nano Letters* **14**, 6231 (2014), pMID: 25302768, <https://doi.org/10.1021/nl502557g>.
- [37] H. H. Huang, X. Fan, D. J. Singh, H. Chen, Q. Jiang, and W. T. Zheng, *Phys. Chem. Chem. Phys.* **18**, 4086 (2016).
- [38] D. Alfè, *Computer Physics Communications* **180**, 2622 (2009).
- [39] A. Kokalj, *Journal of Molecular Graphics and Modelling* **17**, 176 (1999).
- [40] K. Momma and F. Izumi, *Journal of Applied Crystallography* **44**, 1272 (2011).
- [41] X.-B. Li, X. Q. Liu, X. Liu, D. Han, Z. Zhang, X. D. Han, H.-B. Sun, and S. B. Zhang, *Phys. Rev. Lett.* **107**, 015501 (2011).
- [42] D. Erben, A. Steinhoff, M. Lorke, and F. Jahnke, *Optical nonlinearities in the excited carrier density of atomically thin transition metal dichalcogenides* (2020), arXiv:2012.07642 [cond-mat.mes-hall].
- [43] A. Laturia, M. L. Van de Put, and W. G. Vandenberghe, *npj 2D Materials and Applications* **2**, 6 (2018).
- [44] T. Sohler, M. Calandra, and F. Mauri, *Phys. Rev. B* **96**, 075448 (2017).
- [45] N. Marzari, D. Vanderbilt, A. De Vita, and M. C. Payne, *Phys. Rev. Lett.* **82**, 3296 (1999).
- [46] A. V. Kolobov, P. Fons, and J. Tominaga, *Phys. Rev. B* **94**, 094114 (2016).
- [47] A. Krishnamoorthy, L. Bassman, R. K. Kalia, A. Nakano, F. Shimojo, and P. Vashishta, *Nanoscale* **10**, 2742 (2018).
- [48] Q. Song, H. Wang, X. Xu, X. Pan, Y. Wang, F. Song, X. Wan, and L. Dai, *RSC Adv.* **6**, 103830 (2016).
- [49] J. Lee, F. Ye, Z. Wang, R. Yang, J. Hu, Z. Mao, J. Wei, and P. X.-L. Feng, *Nanoscale* **8**, 7854 (2016).
- [50] Y. Cao, N. Sheremetyeva, L. Liang, H. Yuan, T. Zhong, V. Meunier, and M. Pan, *2D Materials* **4**, 035024 (2017).
- [51] Y. Kim, Y. I. Jhon, J. Park, J. H. Kim, S. Lee, and Y. M. Jhon, *Nanoscale* **8**, 2309 (2016).
- [52] W. Yang, Z.-Y. Yuan, Y.-Q. Luo, Y. Yang, F.-W. Zheng, Z.-H. Hu, X.-H. Wang, Y.-A. Liu, and P. Zhang, *Phys. Rev. B* **99**, 235401 (2019).
- [53] M. Calandra, *Phys. Rev. B* **88**, 245428 (2013).
- [54] D. Yang, S. J. Sandoval, W. M. R. Divigalpitiya, J. C. Irwin, and R. F. Frindt, *Phys. Rev. B* **43**, 12053 (1991).
- [55] B. Peng, H. Zhang, W. Chen, B. Hou, Z.-J. Qiu, H. Shao, H. Zhu, B. Monserrat, D. Fu, H. Weng, and C. M. Soukoulis, *npj 2D Materials and Applications* **4**, 14 (2020).
- [56] C. Si, D. Choe, W. Xie, H. Wang, Z. Sun, J. Bang, and S. Zhang, *Nano Letters* **19**, 3612 (2019), pMID: 31096752, <https://doi.org/10.1021/acs.nanolett.9b00613>.
- [57] C. H. Naylor, W. M. Parkin, J. Ping, Z. Gao, Y. R. Zhou, Y. Kim, F. Streller, R. W. Carpick, A. M. Rappe, M. Drndić, J. M. Kikkawa, and A. T. C. Johnson, *Nano Letters* **16**, 4297 (2016), pMID: 27223343, <https://doi.org/10.1021/acs.nanolett.6b01342>.
- [58] Y. C. Jiang, J. Gao, and L. Wang, *Scientific Reports* **6**, 19624 (2016).
- [59] A. Kumar and P. K. Ahluwalia, *Physica B Condensed Matter* **407**, 4627 (2012).
- [60] In Ref.[59] the intensity of the monolayer dielectric function is incorrectly renormalized due to the presence of the vacuum, an effect that in the paper is incorrectly attributed to the reduced number of bands.
- [61] J. Ma, Y. Chen, Z. Han, and W. Li, *2D Materials* **3**, 045010 (2016).